View metadata, citation and similar papers at core.ac.uk
brought to you by CORE
provided by Elsevier - Publisher Connector

Ain Shams Engineering Journal (2015) 6, 511–530

Ain Shams University
Ain Shams Engineering Journal
www.elsevier.com/locate/asej
www.sciencedirect.com

ELECTRICAL ENGINEERING

DE optimized fuzzy PID controller with derivative filter for LFC of multi source power system in deregulated environment

Rabindra Kumar Sahu *, G.T. Chandra Sekhar, Sidhartha Panda

Department of Electrical Engineering, Veer Surendra Sai University of Technology (VSSUT), Burla 768018, Odisha, India

Received 5 June 2014; revised 6 December 2014; accepted 11 December 2014
Available online 29 January 2015

KEYWORDS

Load Frequency Control (LFC);
Differential Evolution algorithm (DE);
Fuzzy Logic Controller (FLC);
Generation Rate Constraint (GRC);
HVDC link;
Sensitivity analysis

Abstract In this paper, Differential Evolution (DE) optimized fuzzy PID controller with derivative Filter (PIDF) is proposed for Load Frequency Control (LFC) of a deregulated power system with multi-source power generation and interconnected via parallel AC/DC transmission links. To get an accurate insight of the LFC problem, important physical constraints such as time delay and GRC are considered. The performance of proposed controller is evaluated at all possible power transactions that take place in a deregulated power market. The improvement in dynamic performance of the power system with DC link in parallel with AC tie-line is also assessed. Further, sensitivity analysis is performed by varying the system parameters and operating load conditions from their nominal values. It is observed from the simulation results that the optimum gains of the proposed controller need not be reset even if the system is subjected to wide variation in loading condition and system parameters.
© 2015 Faculty of Engineering, Ain Shams University. Production and hosting by Elsevier B.V. This is an open access article under the CC BY-NC-ND license (http://creativecommons.org/licenses/by-nc-nd/4.0/).

1. Introduction

Modern power systems consist of a large number of control areas with diverse sources of generation, which generate power to meet the load demand. However, mismatch between generated power and demand results in the deviation in the system frequency from its nominal value. This also creates undesired exchange of power between control areas. The problem of controlling the real power output of generating units in response to changes in system frequency and tie-line power interchange within specified limits is known as Load Frequency Control (LFC) [1]. LFC is one of the important control problems in an interconnected power system design and operation, and is becoming more significant today due to the increasing size, changing structure, emerging renewable energy sources and new uncertainties, environmental constraints, and complexity of power systems [2–4].

In recent times, applications of power electronics devices in AC power systems provide attractive benefits of economics and innovative technologies. In particular, High Voltage

* Corresponding author. Tel.: +91 9439702316.
E-mail addresses: rksahu123@gmail.com (R.K. Sahu), gtchsekhar@gmail.com (G.T. Chandra Sekhar), panda_sidhartha@rediffmail.com (S. Panda).
Peer review under responsibility of Ain Shams University.

ELSEVIER Production and hosting by Elsevier

http://dx.doi.org/10.1016/j.asej.2014.12.009
2090-4479 © 2015 Faculty of Engineering, Ain Shams University. Production and hosting by Elsevier B.V.
This is an open access article under the CC BY-NC-ND license (http://creativecommons.org/licenses/by-nc-nd/4.0/).

Nomenclature

apf_k	area participation factor of kth generating unit
b_g	gas turbine constant of valve positioner
B_i	frequency bias parameter of area i (p.u. MW/Hz)
c_g	gas turbine valve positioner
cpf_{kl}	contract participation factor between kth GENCO and lth DISCO
CR	crossover probability
F	nominal system frequency (Hz)
FC	step size
G	number of generation
i	subscript referred to area i (1, 2)
K_{DC}	HVDC power system gain (Hz/p.u.)
K_{PS}	power system gain (Hz/p.u. MW)
K_R	steam turbine reheat constant
N_P	number of population size
P_{Ri}	rated power of area i (MW)
R_G, R_{HY}, R_{TH}	governor speed regulation parameter of gas, hydro and thermal areas respectively (Hz/p.u. MW)
t_{sim}	simulation time (s)
T_{CD}	gas turbine compressor discharge volume-time constant (s)
T_{CR}	gas turbine combustion reaction time delay (s)
T_{DC}	HVDC power system time constant (s)
T_F	gas turbine fuel time constant (s)
T_{GH}	hydro turbine speed governor main servo time constant (s)
T_{PS}	power system time constant (s)
T_R	steam turbine reheat time constant (s)
T_{RH}	hydro turbine speed governor transient droop time constant (s)
T_{RS}	hydro turbine speed governor reset time (s)
T_{SG}	speed governor time constant for thermal areas (s)
T_T	steam turbine time constant (s)
T_W	nominal starting time of water in penstock (s)
T_{12}	synchronizing coefficient between areas 1 and 2 (p.u.)
U_k	control signal to the kth generating unit
X_G	gas governor lead time constant (s)
Y_G	gas governor lag time constant (s)
ΔF_i	incremental change in frequency of area i (Hz)
ΔP_{D_i}	incremental step load change in area i
ΔP_{gk}	incremental change in power output of kth generating unit (p.u. MW)
$\Delta P_{Tie,12}$	incremental change in tie-line power between areas 1 and 2 (p.u.)
$\Delta P_{tie,12}^{actual}$	actual tie-line power between areas 1 and 2 (p.u. MW)
$\Delta P_{tie,12}^{error}$	tie-line power error between areas 1 and 2 (p.u. MW)
$\Delta P_{tie,12}^{scheduled}$	scheduled tie-line power between areas 1 and 2 (p.u. MW)

Direct Current transmission link (HVDC link) in parallel with an AC link interconnecting two control areas, has emerged as an alternative link in the power system scenario, due to its major advantages in meeting these requirements, including long distance overhead bulk power transmission. One more advantage of the HVDC link is that the DC power flow on the line is highly adjustable. Therefore, power flow oscillations in an AC system due to system disturbances can be effectively damped by controlling the DC power and it has been applied widely in operating a DC link in parallel with an AC link interconnecting control areas in order to improve the dynamic performance of system [5]. In many practical situations, a single control area may have many diverse sources of power generation such as thermal, hydro, and gas. Therefore, this work presents a comprehensive study on dynamic performance of a more realistic power system by considering diverse sources of power generation in the control areas interconnected via parallel AC/DC transmission links.

In a conventional power system configuration, the generation, transmission and distribution is owned by a sole entity called Vertically Integrated Utility (VIU), which supplies power to the clients at regulated rates. All such control areas are interconnected by tie lines. Following a load disturbance within an area, the frequency of that area experiences a transient change, and the feedback mechanism comes into play which in turn generates an appropriate rise/lower signal to the turbine toward eliminate the mismatch between generations and loads. In steady state, the generation is matched with the load, driving the tie line power and frequency deviations to zero. In the restructured power systems, the VIU of conventional power system no longer exists. However, the common objectives, i.e. restoring the frequency and the net interchanges of power between control areas to their desired values for each control area are remained [6]. In an open energy market, Generating Companies (GENCOs) may or may not participate in the LFC task as they are independent power utilities. On the other hand, Distribution Companies (DISCOs) may contract with GENCOs, renewable power plants, or Independent Power Producers (IPPs) for the transaction of power in different areas [7]. Thus, in restructured environment, control is greatly decentralized and Independent System Operators (ISOs) are responsible for maintaining the system frequency and tie-line power flows. Many articles on isolated and interconnected power system concerning with LFC issues under deregulated environment have been reported in the literature [6–10]. Chidambaram and Paramasivam [11] have proposed LFC strategy for a two- area multi-units power system under deregulated environment in the presence of Redox Flow Batteries (RFB) and Interline Power Flow Controller (IPFC). Recently, Parmar et al. [12] have studied the multi-source power generation in deregulated power environment using optimal output feedback controller. However, in the above literatures the effect of physical constraints such as Time Delay (TD) and Generation Rate Constraint (GRC) is not examined which needs further comprehensive study.

It has been reported by many researchers that Fuzzy Logic Controller (FLC) improves the closed loop performance of PI/PID controller and can handle any changes in operating point or in system parameter by online updating the controller parameters [13–15]. Fuzzy logic based PID controller can be successfully used for all nonlinear system but there is no specific mathematical formulation to decide the proper choice of fuzzy parameters (such as inputs, scaling factors, membership functions and rule base). Normally these parameters are selected by using certain empirical rules and therefore may not be the optimal parameters. Improper selection of input–output scaling factor may affect the performance of FLC to a greater extent. Classical techniques of determining the optimum gains of the fuzzy PIDF controller are time consuming and may fail to give optimal solution. Differential Evolution (DE) being a global optimizing method is designed to explore the search space and most likely gives an optimal/near-optimal solution.

In view of the above, a maiden attempt has been made in the present paper to tune the input and output scaling factors of fuzzy PIDF controller using DE optimization technique for LFC of multisource power systems in the presence of physical constraints. The aim of the present work can be summarized as follows:

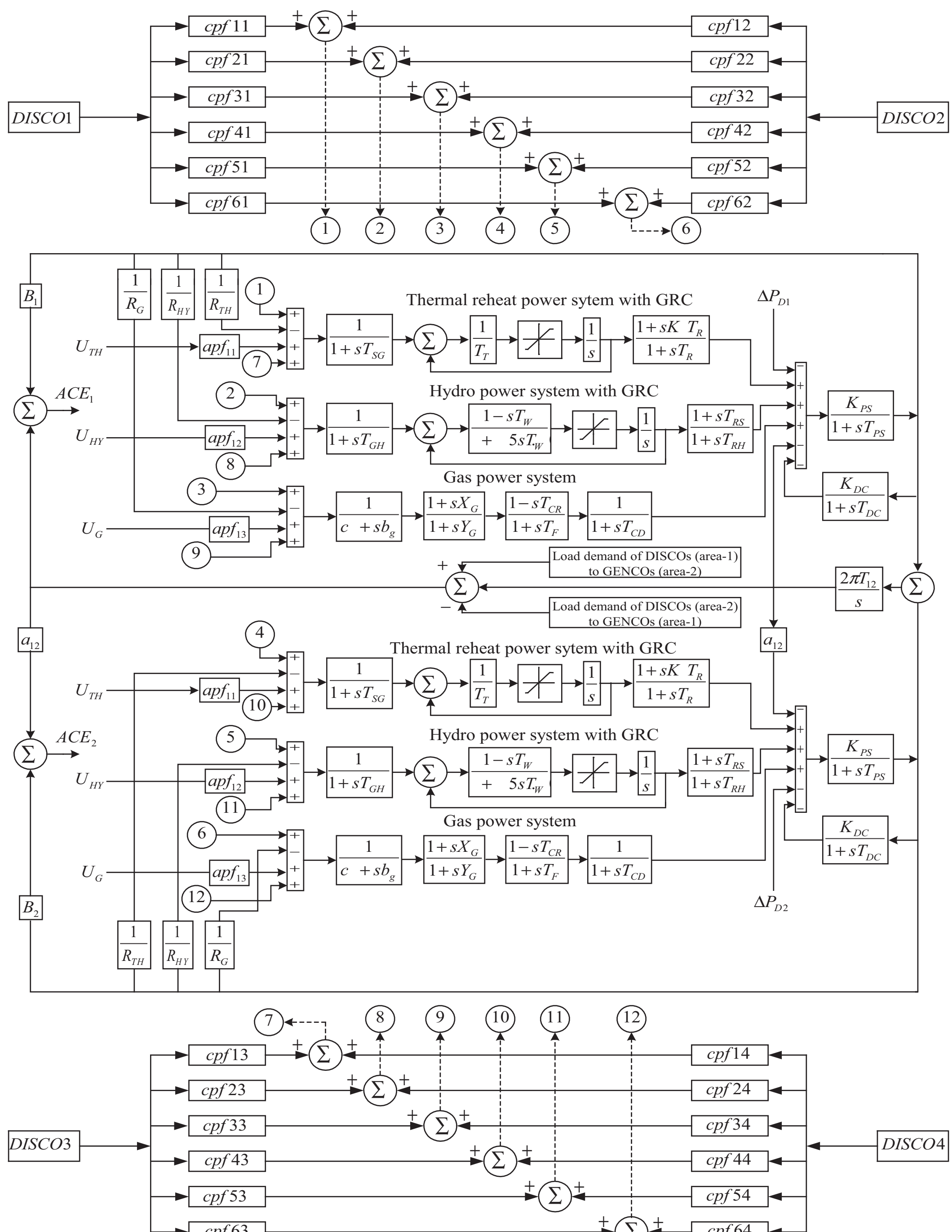

Figure 1 Block diagram of multi-area multi-source interconnected power system with HVDC link.

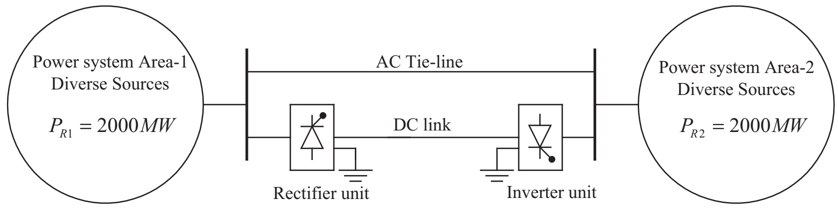

Figure 2 Two-area interconnected power system with HVDC link in parallel with an AC link.

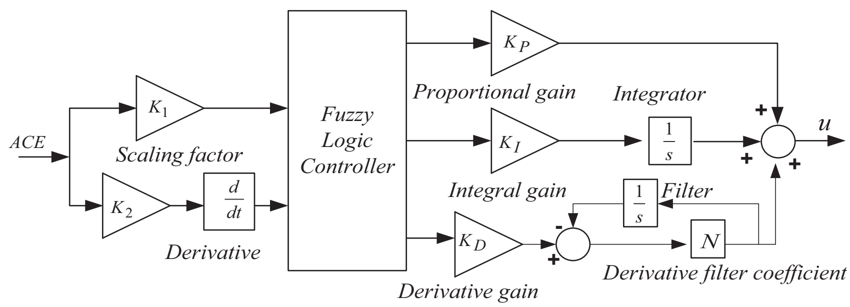

Figure 3 Structure of proposed fuzzy PIDF controller.

(i) To design a fuzzy PIDF controller employing DE optimization technique.
(ii) To study the effect of proposed controller under at all possible power transactions scenario.
(iii) To assess the effect of using DC link in parallel with AC tie-line on the dynamic performance of the power system.
(iv) To investigate the capabilities of proposed controllers under wide variation in system parameters and loading conditions.

2. Material and method

2.1. Power system under study

The system under investigation consists of two area six units interconnected thermal, hydro and gas power system as shown in Fig. 1. Each area has a rating of 2000 MW with a nominal load of 1640 MW. The system is widely used in the literature for the design and analysis of automatic load frequency control of interconnected areas [5,12]. The control areas 1 and 2 comprise of reheat thermal, hydro and gas power system as shown in Fig. 1. Each control area has its regulation parameter and participation factor which decide the contribution to the nominal loading. The load contribution of each generating station in each area is taken as thermal 985 MW, hydro 490 MW and gas 165 MW. To get an accurate insight of the LFC problem, it is essential to include the important inherent requirement and the basic physical constraints and include the model. The important constraints which affect the power system performance are Time Delay (TD) and Generation Rate Constraint (GRC). In view of the above, the TD and GRC are incorporated in power system model as shown in Fig. 1. Owing to the growing complexity of power systems in deregulated environment, communication delays become a significant challenge in the LFC analysis. Time delays can degrade a system's performance and even cause system instability. In the present paper, a time delay of 50 ms is considered [16]. In a power system having steam plants, power generation can change only at a specified maximum rate. In thermal power plants, power generation can change only at a specified maximum/minimum rate known as GRC. In the present study, a GRC of 3% per min for thermal units and 270% per minute for rising and 360% per minute for lowering generation in hydro areas are considered [17]. The relevant parameters are given in Appendix A.

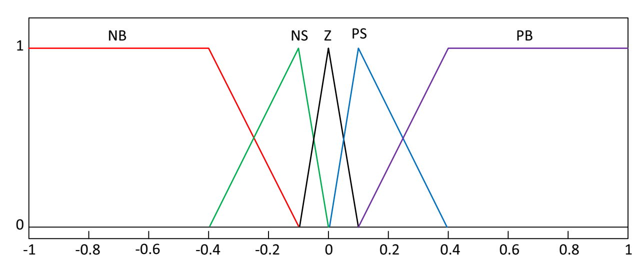

Figure 4 Membership functions for error, error derivative and FLC output.

Table 1 Rule base for error, derivative of error and FLC output.

e	$\dot{e}$				
	NB	NS	Z	PS	PB
NB	NB	NB	NS	NS	Z
NS	NB	NS	NS	Z	PS
Z	NS	NS	Z	PS	PS
PS	NS	Z	PS	PS	PB
PB	Z	PS	PS	PB	PB

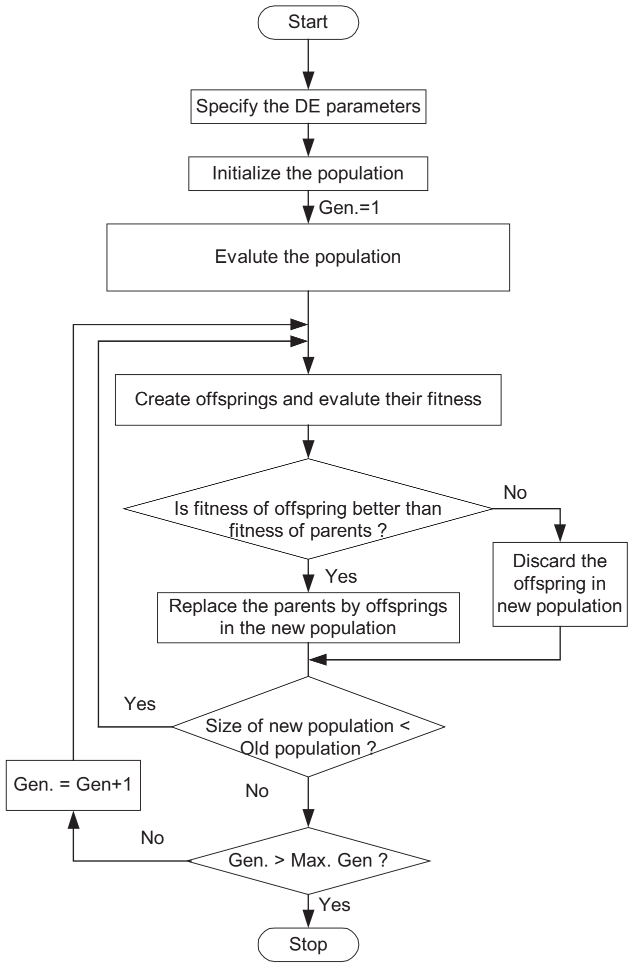

Figure 5 Flow chart of DE optimization approach.

2.2. Modeling of LFC in restructured environment with HVDC link

In the restructured power system, GENCOs sell power to various DISCOs at competitive prices. Thus, DISCOs have the freedom to choose the GENCOs for contracts. They may or may not have contracts with the GENCOs in their own area. The LFC in a deregulated electricity market should be designed to consider different types of possible transactions, such as Poolco-based transactions, bilateral transactions and a combination of these two. The various combinations of contracts between DISCOs and GENCOs which can be easily visualized by the concept of DISCO Participation Matrix (DPM) [12]. The rows of DPM correspond to GENCOs and columns to DISCOs which contract power. Each entry in this matrix can be thought as a fraction of total load contracted by *l*th-DISCO (column) toward *k*th-GENCO (row). The sum of all the entries in a column in this matrix is unity. So, mathematically it can be expressed as

$$\sum_{k}^{n} \mathrm{cpf}_{kl} = 1 \tag{1}$$

where 'cpf' represents "contract participation factor" i.e. p.u. MW load of a corresponding DISCO.

In the present study, two control areas are considered. Each control area comprises of three GENCOs and two DISCOs as shown in Fig. 1. Let GENCO1, GENCO2, GENCO3, DISCO1 and DISCO2 be in area-1 and GENCO4, GENCO5, GENCO6, DISCO3 and DISCO4 be in area-2. The corresponding DPM for the system will have the structure as given below:

$$\mathrm{DPM} = \begin{bmatrix} \mathrm{cpf}_{11} & \mathrm{cpf}_{12} & \mathrm{cpf}_{13} & \mathrm{cpf}_{14} \\ \mathrm{cpf}_{21} & \mathrm{cpf}_{22} & \mathrm{cpf}_{23} & \mathrm{cpf}_{24} \\ \mathrm{cpf}_{31} & \mathrm{cpf}_{32} & \mathrm{cpf}_{33} & \mathrm{cpf}_{34} \\ \mathrm{cpf}_{41} & \mathrm{cpf}_{42} & \mathrm{cpf}_{43} & \mathrm{cpf}_{44} \\ \mathrm{cpf}_{51} & \mathrm{cpf}_{52} & \mathrm{cpf}_{53} & \mathrm{cpf}_{54} \\ \mathrm{cpf}_{61} & \mathrm{cpf}_{62} & \mathrm{cpf}_{63} & \mathrm{cpf}_{64} \end{bmatrix} \tag{2}$$

Table 2 Tuned PIDF/fuzzy PIDF controller parameters for Poolco based transaction.

Controller parameters		Without HVDC link		With HVDC link
		PIDF	Fuzzy PIDF	Fuzzy PIDF
Thermal	K_1	–	0.1491	0.8952
	K_2	–	0.9601	1.9675
	K_{P1}	−1.9898	−1.3823	−1.5003
	K_{I1}	−0.6069	−0.8762	−1.2579
	K_{D1}	0.0764	−0.9628	0.2114
	N_1	140.5037	167.7958	224.9104
Hydro	K_3	–	1.0774	1.4176
	K_4	–	1.7246	1.9899
	K_{P2}	1.7948	0.3555	−0.3757
	K_{I2}	0.2576	−1.3767	1.0659
	K_{D2}	−0.6571	−1.6815	−0.5664
	N_2	81.8396	189.4217	65.0361
Gas	K_5	–	0.5850	0.2671
	K_6	–	0.0082	0.0331
	K_{P3}	−0.7315	0.5172	−1.9539
	K_{I3}	0.2576	−1.3767	1.0659
	K_{D3}	1.3321	−1.8177	−0.7417
	N_3	239.9045	118.0382	112.9930

Table 3 Performance index values under Poolco based transaction.

Parameters		PIDF without HVDC	Fuzzy PIDF without HVDC	Fuzzy PIDF with HVDC
ITAE		90.3614	5.0255	2.3132
T_S (s)	ΔF_1	100.00	15.56	7.64
	ΔF_2	100.00	16.95	11.18
	ΔP_{Tie}	30.65	12.18	08.66
Peak overshoot ($\times 10^{-3}$)	ΔF_1	40.938	21.992	1.1096
	ΔF_2	49.420	5.1118	1.8031
	ΔP_{Tie}	8.8161	5.5659	1.8349
Peak undershoot ($\times 10^{-3}$)	ΔF_1	−247.220	−220.957	−116.224
	ΔF_2	−159.629	−126.750	−25.214
	ΔP_{Tie}	−43.263	−37.654	−16.741

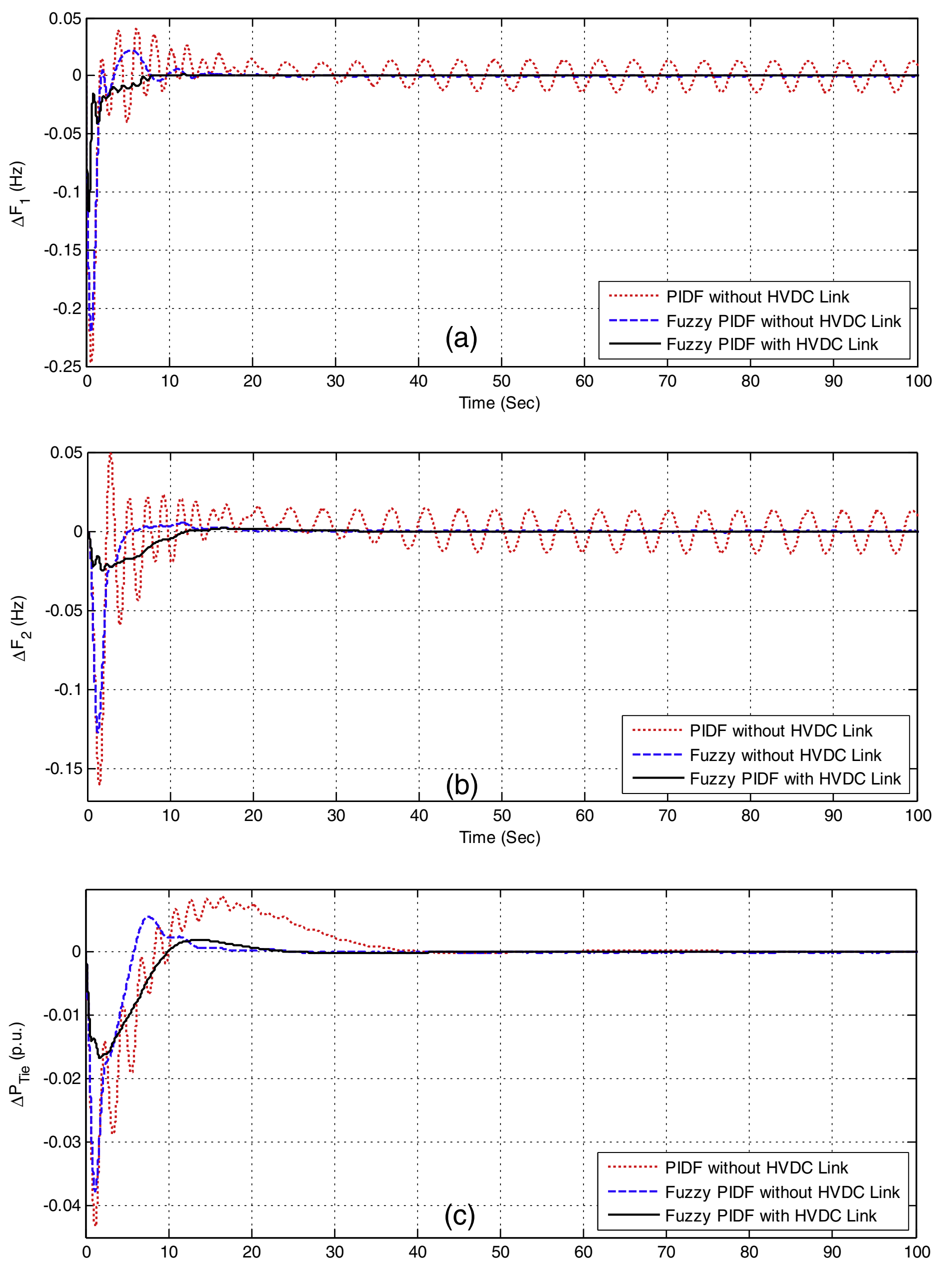

Figure 6 Dynamic responses of the system for Poolco based transaction. (a) Frequency deviation of area-1. (b) Frequency deviation of area-2. (c) Tie line power deviation.

The scheduled steady state power flow on the tie-line can be given as:

$$\Delta P_{tie,12}^{scheduled} = (\text{Demand of DISCOs in area 1 to GENCOs in area 2}) - (\text{Demand of DISCOs in area2 to GENCOs in area 1}) \quad (3)$$

Mathematically Eq. (3) can be defined as:

$$\Delta P_{tie,12}^{scheduled} = \sum_{k=1}^{3}\sum_{l=3}^{4} \text{cpf}_{kl}\Delta P_{Ll} - \sum_{k=4}^{6}\sum_{l=1}^{2} \text{cpf}_{kl}\Delta P_{Ll} \quad (4)$$

The actual tie-line power can be represented as:

$$\Delta P_{tie,12}^{actual} = \frac{2\pi T_{12}}{s}(\Delta F_1 - \Delta F_2) \quad (5)$$

The tie-line power error can now be expressed as:

$$\Delta P_{tie,12}^{error} = \Delta P_{tie,12}^{actual} - \Delta P_{tie,12}^{scheduled} \quad (6)$$

$\Delta P_{tie,12}^{error}$ reduces to zero in the steady as the actual tie-line power flow reaches the scheduled power flow. The generated power or contracted power supplied by the GENCOs is given as

$$\Delta P_{gk} = \sum_{l=1}^{4} \text{cpf}_{kl} P_{Ll} \quad (7)$$

This error signal is used to generate the respective Area Control Error (ACE) signals during the traditional scenario as given below:

$$\text{ACE}_1 = B_1\Delta F_1 + \Delta P_{tie,12}^{error} \quad (8)$$

$$\text{ACE}_2 = B_2\Delta F_2 + \Delta P_{tie,21}^{error} \quad (9)$$

As there are two GENCOs in each area, ACE signal has to be distributed among them in proportion to their participation in the LFC. Coefficients that distribute ACE to GENCOs are termed as "ACE Participation Factors (apfs)". In a given control area, the sum of participation factors is equal to 1. Hence,

Table 4 Tuned PIDF/fuzzy PIDF controller parameters for bilateral based transaction.

Controller parameters		Without HVDC link		With HVDC link
		PIDF	Fuzzy PIDF	Fuzzy PIDF
Thermal	K_1	–	0.1879	0.4363
	K_2	–	0.5392	0.4574
	K_{P1}	−1.9135	−1.6870	−0.7199
	K_{I1}	−1.1667	−1.5397	−1.2687
	K_{D1}	0.8395	−1.0708	−0.2154
	N_1	32.2996	86.9730	193.2675
Hydro	K_3	–	0.3929	0.7542
	K_4	–	0.8350	1.5580
	K_{P2}	1.9642	−0.5917	−1.0338
	K_{I2}	−1.4455	−0.0302	0.0114
	K_{D2}	0.7114	−1.2024	−0.9366
	N_2	251.2895	183.0175	231.9807
Gas	K_5	–	0.0360	1.0397
	K_6	–	0.3839	0.2785
	K_{P3}	−0.8935	−0.5867	1.6856
	K_{I3}	−1.4455	−0.0302	0.0114
	K_{D3}	0.0492	0.9715	0.6743
	N_3	193.1864	43.7821	141.3462

Table 5 Performance index values under bilateral based transaction.

Parameters		Bilateral based		
		PIDF without HVDC	Fuzzy PIDF without HVDC	Fuzzy PIDF with HVDC
ITAE		69.16	13.19	3.28
T_S (s)	ΔF_1	96.99	60.13	19.39
	ΔF_2	92.60	44.72	19.36
	ΔP_{Tie}	03.50	03.15	02.60
Peak overshoot ($\times 10^{-3}$)	ΔF_1	76.440	13.661	7.529
	ΔF_2	77.132	12.621	7.123
	ΔP_{Tie}	1.2225	0.2801	0.988
Peak undershoot ($\times 10^{-3}$)	ΔF_1	−329.68	−270.739	−113.457
	ΔF_2	−339.06	−276.970	−113.508
	ΔP_{Tie}	−3.340	−3.340	−3.340

apf_{11}, apf_{12}, and apf_{13} are considered as ACE participation factor in area 1 and apf_{21}, apf_{22}, and apf_{23} are in area 2. In order to improve the dynamic performance of the power system, a HVDC link is considered in parallel with HVAC system. The single line diagram of two area power system with parallel HVAC/HVDC links is shown in Fig. 2 [6]. When a step load disturbance is applied in an area, the control system of HVDC link reacts quickly to suppress the peak value of transient frequency deviation. Subsequently, the steady state errors of the frequency deviation are eliminated by the governors. For simplicity, the dynamics of governors in both areas can be neglected in the control design of HVDC link. For sudden step load perturbation, the change in output in area-1 of a HVDC link can be given as:

$$\Delta P_{DC} = \frac{K_{DC}}{1 + sT_{DC}} \Delta F_1 \tag{10}$$

where K_{DC} is gain of a HVDC link and T_{DC} is time constant of HVDC link in seconds.

2.3. Controller structure and objective function

Classical PID controllers are used in most of the industrial processes due to their simple and robust design, low cost, and effectiveness for linear systems. However, the classical PID controllers are usually not effective due to their linear structure, especially, if the processes involved are higher order, time delay systems and systems with uncertainties. On the

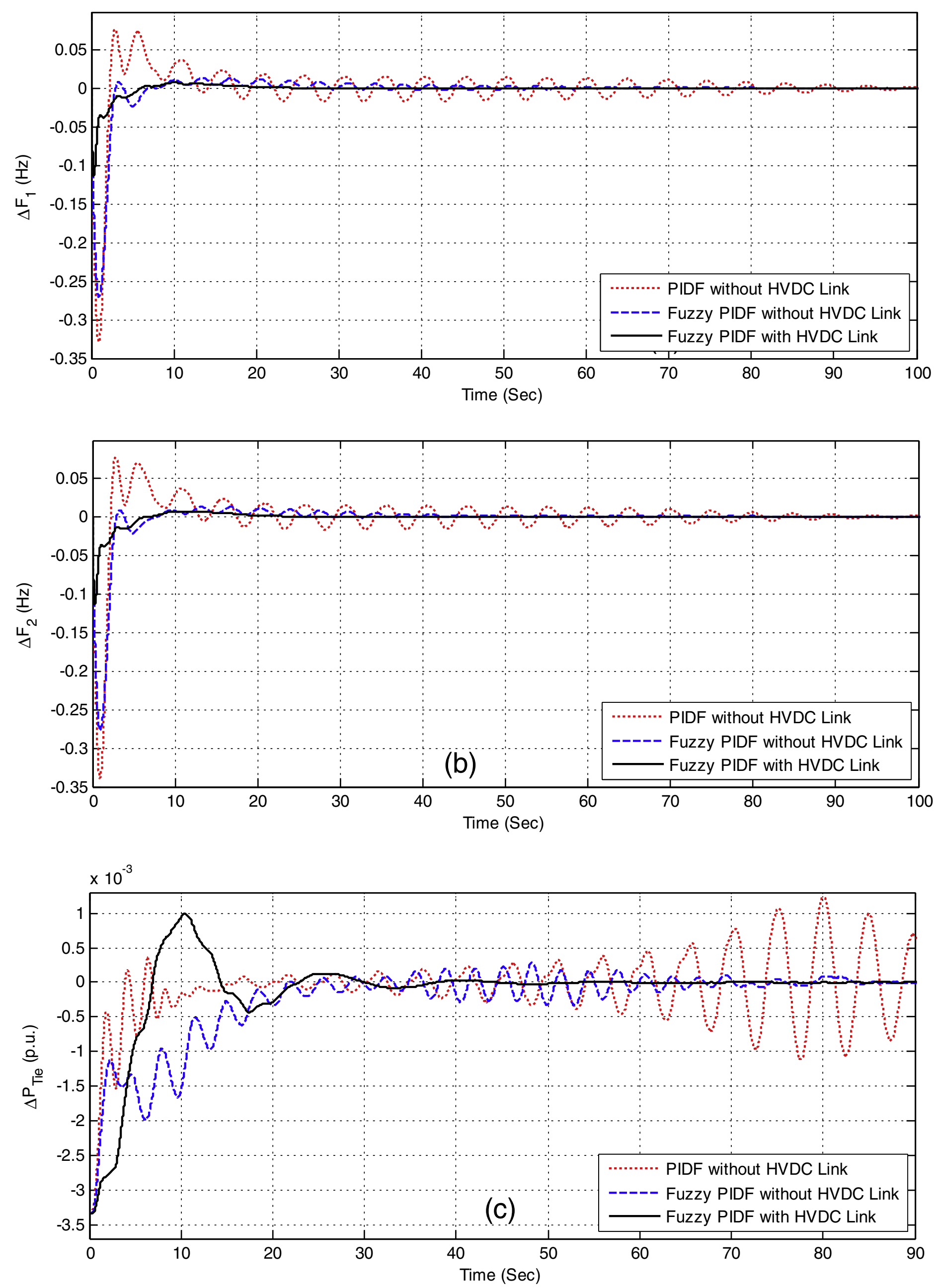

Figure 7 Dynamic responses of the system for bilateral based transaction. (a) Frequency deviation of area-1. (b) Frequency deviation of area-2. (c) Tie line power deviation.

other hand, the Fuzzy Logic Controller (FLC) in a closed loop control system is basically a static non-linearity between its inputs and outputs, which can be tuned easily to match the desired performance of the control system in a more heuristic manner. It has been shown by many contemporary researchers that application of FLC enhances the closed loop performance of a conventional PI controller in terms of handling change in an operating point by online updating the controller parameters [13,14]. Fuzzy control tuning by rule tuning and membership function (MF) tuning is a very difficult task and may not be effective. As gain tuning greatly affects the performance, it is the most common way of tuning the fuzzy control. So general and robust rule base and standard MF's can be used for different applications and scaling factors can be tuned for optimum fuzzy PI control [18]. However, fuzzy PI controllers may show poor performance during the transient phase for higher order processes due to their internal integration operation. To obtain overall improved performance, fuzzy PID controllers are suggested [19,20]. However, when the input signal has sharp corners, the derivative term will produce unreasonable size control inputs to the plant. Also, any noise in the control input signal will result in large plant input signals. These reasons often lead to complications in practical applications. The practical solution to these problems is to put a first filter on the derivative term and tune its pole so that the chattering due to the noise does not occur since it attenuates high frequency noise. In view of the above fuzzy Proportional Integral Derivative controller with derivative Filter (PIDF) is chosen in this paper to solve the LFC problem. The structure of fuzzy PIDF controller is shown in Fig. 3. The structure of the fuzzy PID used here is inherited from a combination of fuzzy PI and fuzzy PD controllers from [13], with K_1 and K_2 are input scaling factors of FLC. The FLC output is multiplied K_P, its integral, derivative and filter coefficient are multiplied K_I, K_D and N respectively, and then summed to give the total controller output. In the present paper, fuzzy PIDF controllers are considered for each unit. Therefore three fuzzy PIDF controllers are considered. As equal areas are assumed the test system, similar fuzzy PIDF controllers are assumed for each area.

Table 6 Tuned PIDF/fuzzy PIDF controller parameters for contract violation based transaction.

Controller parameters		Without HVDC link		With HVDC link
		PIDF	Fuzzy PIDF	Fuzzy PIDF
Thermal	K_1	–	0.7134	0.1879
	K_2	–	0.5494	0.5392
	K_{P1}	−1.6109	−1.0066	−1.6870
	K_{I1}	−0.0080	−0.9542	−1.5397
	K_{D1}	−1.4905	−0.0204	1.0708
	N_1	46.3707	98.2769	86.9730
Hydro	K_3	–	0.5288	0.3929
	K_4	–	1.4890	0.8350
	K_{P2}	1.9425	0.8947	−0.5917
	K_{I2}	1.6558	−1.2424	−0.0302
	K_{D2}	−1.9027	−1.8680	1.2024
	N_2	202.6668	109.4254	183.0175
Gas	K_5	–	0.2634	0.0360
	K_6	–	1.6062	0.3839
	K_{P3}	−1.2095	−0.2705	−0.5867
	K_{I3}	−1.6558	−1.2424	−0.0302
	K_{D3}	−1.2278	−0.5095	0.9715
	N_3	23.1106	201.2089	43.7821

Table 7 Performance index values under contract violation based transaction.

Parameters		Contract violation based		
		PIDF without HVDC	Fuzzy PIDF without HVDC	Fuzzy PIDF with HVDC
ITAE		85.1874	10.9645	8.0228
T_S (s)	ΔF_1	100	98.34	36.73
	ΔF_2	100	98.87	37.53
	ΔP_{Tie}	06.45	06.30	06.00
Peak overshoot ($\times 10^{-3}$)	ΔF_1	31.936	11.222	3.092
	ΔF_2	31.202	9.974	3.083
	ΔP_{Tie}	0.5398	0.5406	0.791
Peak undershoot ($\times 10^{-3}$)	ΔF_1	−329.151	−210.852	−119.157
	ΔF_2	−317.921	−198.743	−110.007
	ΔP_{Tie}	−6.849	−7.377	−5.142

Fuzzy controller uses error (e) and derivative of error ($\dot{e}$) as input signals. The outputs of the fuzzy controllers U_{TH}, U_{HY} and U_G are the control inputs of the power system. The input scaling factors are the tuneable parameters K_1, K_2, K_3, K_4, K_5 and K_6. The proportional, integral and derivative gains of fuzzy controller are represented by K_{P1}, K_{P2}, K_{P3}, K_{I1}, K_{I2}, K_{I3}, K_{D1}, K_{D2} and K_{D3} respectively. N_1, N_2 and N_3 are the derivative filter coefficients. In the present study, fixed membership functions and rule base are assumed for the FLC structure. The input scaling factors (K_1, K_2, K_3, K_4, K_5 and K_6) and output scaling factors (K_{P1}, K_{P2}, K_{P3}, K_{I1}, K_{I2}, K_{I3}, K_{D1}, K_{D2} K_{D3}, N_1, N_2 and N_3) are optimized employing DE algorithm to minimize the objective function.

Usually triangular, trapezoidal and bell shaped membership functions are preferred as their functional representation can be easily achieved; they require minimal memory usage for storage and can be manipulated efficiently by the fuzzy inference engine to meet the stiff limits of real time requirements. Triangular membership function is widely adopted in controller design for real time applications as the parametric practical depiction of the triangular membership function is economical compared to other alternatives. In view of the above, triangular membership functions have been chosen in the present study. Also, from the perspective of computational efficiency, good memory usage and performance analysis requirements, and a uniform representation of the membership

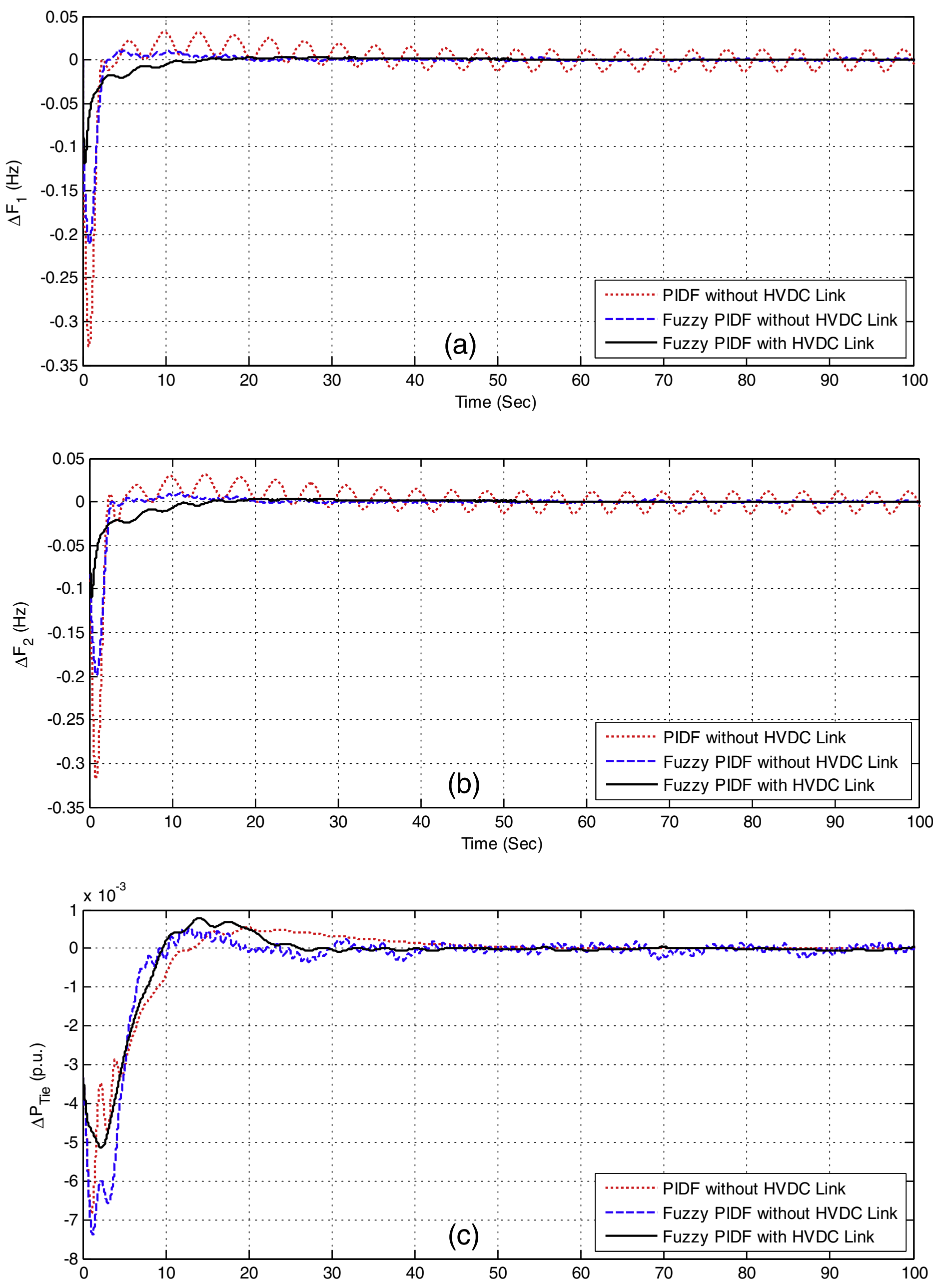

Figure 8 Dynamic responses of the system for contract violation. (a) Frequency deviation of area-1. (b) Frequency deviation of area-2. (c) Tie line power deviation.

function is generally preferred [20]. Hence, the same membership functions are chosen for the error, the error derivative and the FLC output. The membership functions are used with five fuzzy linguistic variables such as NB (negative big), NS (negative small), Z (zero), PS (positive small) and PB (positive big) for both the inputs and the output. Membership functions for error, error derivative and FLC output is shown in Fig. 4. Mamdani fuzzy interface engine is selected for this work. The FLC output is determined by using center of gravity method of defuzzification. The two-dimensional rule base for error, error derivative and FLC output is shown in Table 1.

In the design of a modern heuristic optimization technique based controller, the objective function is first defined based on the desired specifications and constraints. Performance criteria usually considered in the control design are the Integral of Time multiplied Absolute Error (ITAE), Integral of Squared Error (ISE), Integral of Time multiplied Squared Error (ITSE) and Integral of Absolute Error (IAE). ITAE criterion reduces the settling time which cannot be achieved with IAE or ISE based tuning. ITAE criterion also reduces the peak overshoot. ITSE based controller provides large controller output for a sudden change in set point which is not advantageous from controller design point of view. It has been reported in the literature that Integral of Time multiplied Absolute Error (ITAE) gives a better performance compared to other integral based performance criteria [21,22]. Therefore ITAE is used as objective function in this paper to optimize the input scaling factors and output scaling factors. Expression for the ITAE objective function is depicted in Eq. (11).

$$J = ITAE = \int_0^{t_{sim}} (|\Delta F_1| + |\Delta F_2| + |\Delta P_{Tie}|) \cdot t \cdot dt \tag{11}$$

where ΔF_1 and ΔF_2 are the system frequency deviations; ΔP_{Tie} is the incremental change in tie line power; t_{sim} is the time range of simulation.

3. Differential evolution

Differential Evolution (DE) algorithm is a search heuristic algorithm introduced by Storn and Price [23]. It is a simple, efficient, reliable algorithm with easy coding. The main advantage of DE over Genetic Algorithm (GA) is that GA uses crossover operator for evolution while DE relies on mutation operation. The mutation operation in DE is based on the difference of randomly sampled pairs of solutions in the population. An optimization task consisting of D variables can be represented by a D-dimensional vector. A population of N_P solution vectors is randomly initialized within the parameter bounds at the beginning. The population is modified by applying mutation, crossover and selection operators. DE algorithm uses two generations; old generation and new generation of the same population size. Individuals of the current population become target vectors for the next generation. The mutation operation produces a mutant vector for each target vector, by adding the weighted difference between two randomly chosen vectors to a third vector. A trial vector is generated by the crossover operation by mixing the parameters of the mutant vector with those of the target vector. The trial vector substitutes the target vector in the next generation if it obtains a better fitness value than the target vector. The evolutionary operators are described below:

3.1. Initialization of parameter

DE begins with a randomly initiated population of size N_P *of* D dimensional real-valued parameter vectors. Each parameter j lies within a range and the initial population should spread over this range as much as possible by uniformly randomizing individuals within the search space constrained by the prescribed lower bound X_j^L and upper bound X_j^U.

3.2. Mutation operation

For the mutation operation, a parent vector from the current generation is selected (known as target vector), a mutant vec-

Table 8 Sensitive analysis under Poolco based transaction with HVDC link.

Parameter variation	% change	Settling time in (s)			Peak overshoot ($\times 10^{-3}$)			ITAE
		ΔF_1	ΔF_2	ΔP_{Tie}	ΔF_1	ΔF_2	ΔP_{Tie}	
Nominal	0	7.64	11.18	8.66	1.1096	1.8031	1.8349	2.3132
Loading condition	−25	7.65	11.20	8.67	1.1096	1.8031	1.8349	2.3185
	+25	7.64	11.17	8.65	1.1096	1.8031	1.8349	2.3194
T_{SG}	−25	7.66	11.19	8.66	1.0158	1.7516	1.8407	2.7020
	+25	7.63	11.19	8.65	1.1075	1.7948	1.8618	2.2912
T_T	−25	7.63	11.20	8.65	0.9263	1.7338	1.8362	2.8248
	+25	7.64	11.17	8.66	1.1762	1.8297	1.8846	2.3257
T_{RH}	−25	8.82	12.07	9.49	0.9812	1.2741	1.7510	2.3858
	+25	6.80	10.90	8.34	0.8302	1.7469	1.8890	2.2144
T_{CD}	−25	7.45	11.14	8.62	1.0408	1.7896	1.8429	2.2820
	+25	7.75	11.19	8.69	1.3244	1.9221	1.9038	2.4130
T_{12}	−25	7.57	11.45	9.04	1.8260	1.8476	1.8250	2.3502
	+25	7.70	11.05	8.43	0.8660	1.7151	1.8791	2.3449
R	−25	7.48	11.51	8.65	0.5341	1.1708	1.6982	2.1358
	+25	11.80	17.6	15.07	2.0214	2.3693	2.0880	2.7431

tor is obtained by the differential mutation operation (known as donor vector) and finally an offspring is produced by combining the donor with the target vector (known as trial vector). Mathematically it can be expressed as:

$$V_{i,G+1} = X_{r1,G} + \mathrm{FC} \cdot (X_{r2,G} - X_{r3,G}) \quad (12)$$

where $X_{i,G}$ is the given parameter vector, $X_{r1,G}$ $X_{r2,G}$ and $X_{r3,G}$ are randomly selected vector with distinct indices i, $r1$, $r2$ and $r3$, $V_{i,G+1}$ is the donor vector and FC is a constant from (0, 2).

3.3. Crossover operation

After generating the donor vector through mutation the crossover operation is employed to enhance the potential diversity of the population. For crossover operation three parents are selected and the child is obtained by means of perturbation of one of them. In crossover operation a trial vector $U_{i,G+1}$ is obtained from target vector ($X_{i,G}$) and donor vector ($V_{i,G}$). The donor vector enters the trial vector with probability CR given by:

$$U_{j,i,G+1} = \begin{cases} V_{j,i,G+1} & \text{if} \quad rand_{j,i} \leqslant \mathrm{CR} \quad \text{or} \quad j = I_{rand} \\ X_{j,i,G+1} & \text{if} \quad rand_{j,i} > \mathrm{CR} \quad \text{or} \quad j \neq I_{rand} \end{cases} \quad (13)$$

With $rand_{j,i} \sim U(0,1)$, I_{rand} is a random integer from $(1, 2, \ldots D)$ where D is the solution's dimension, i.e. number of control variables. I_{rand} ensures that $V_{i,G+1} \neq X_{i,G}$.

3.4. Selection operation

To keep the population size constant over subsequent generations, selection operation is performed. In this operation the target vector $X_{i,G}$ is compared with the trial vector $V_{i,G+1}$ and

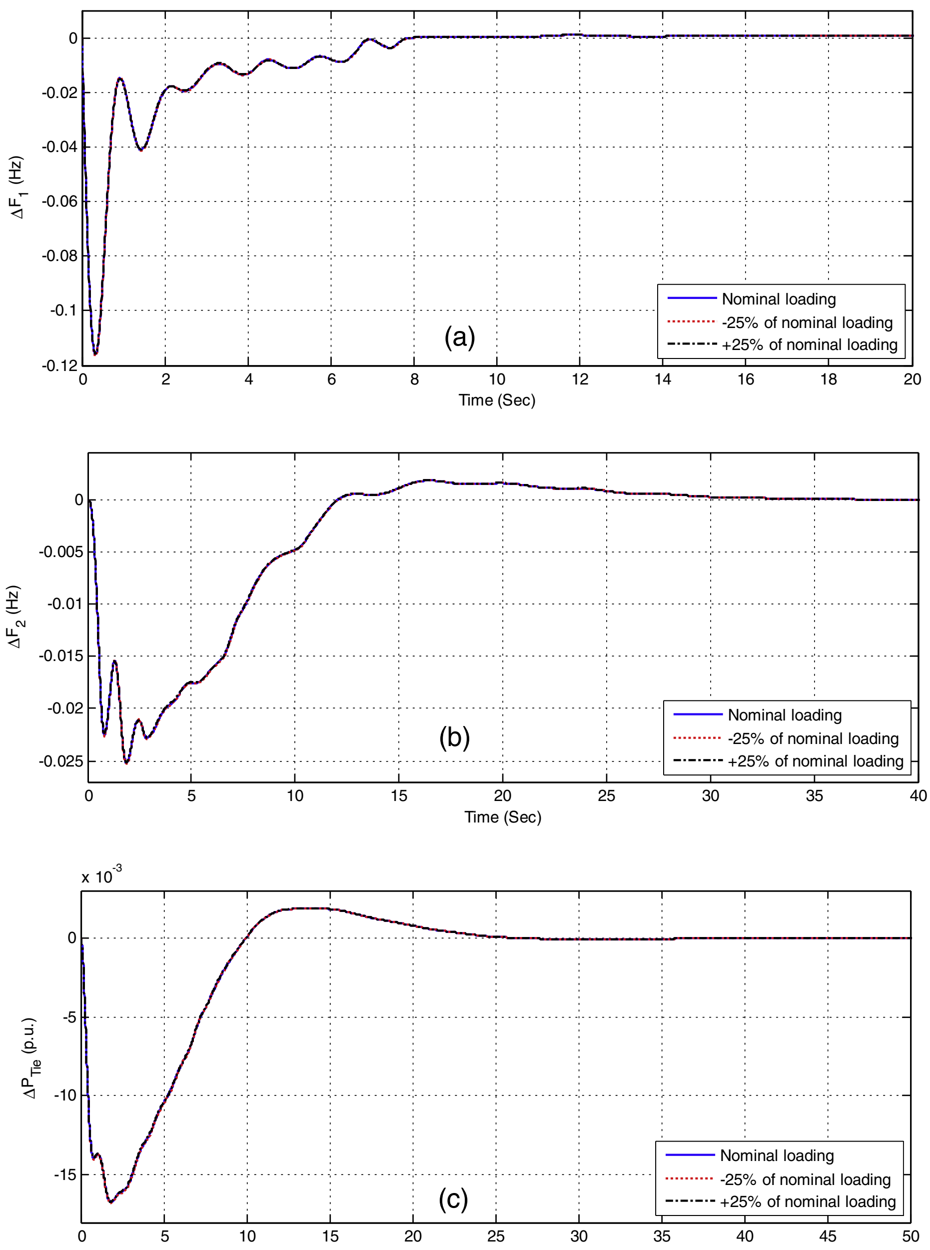

Figure 9 Dynamic responses of the system with variation in nominal loading. (a) Frequency deviation of area-1. (b) Frequency deviation of area-2. (c) Tie line power deviation.

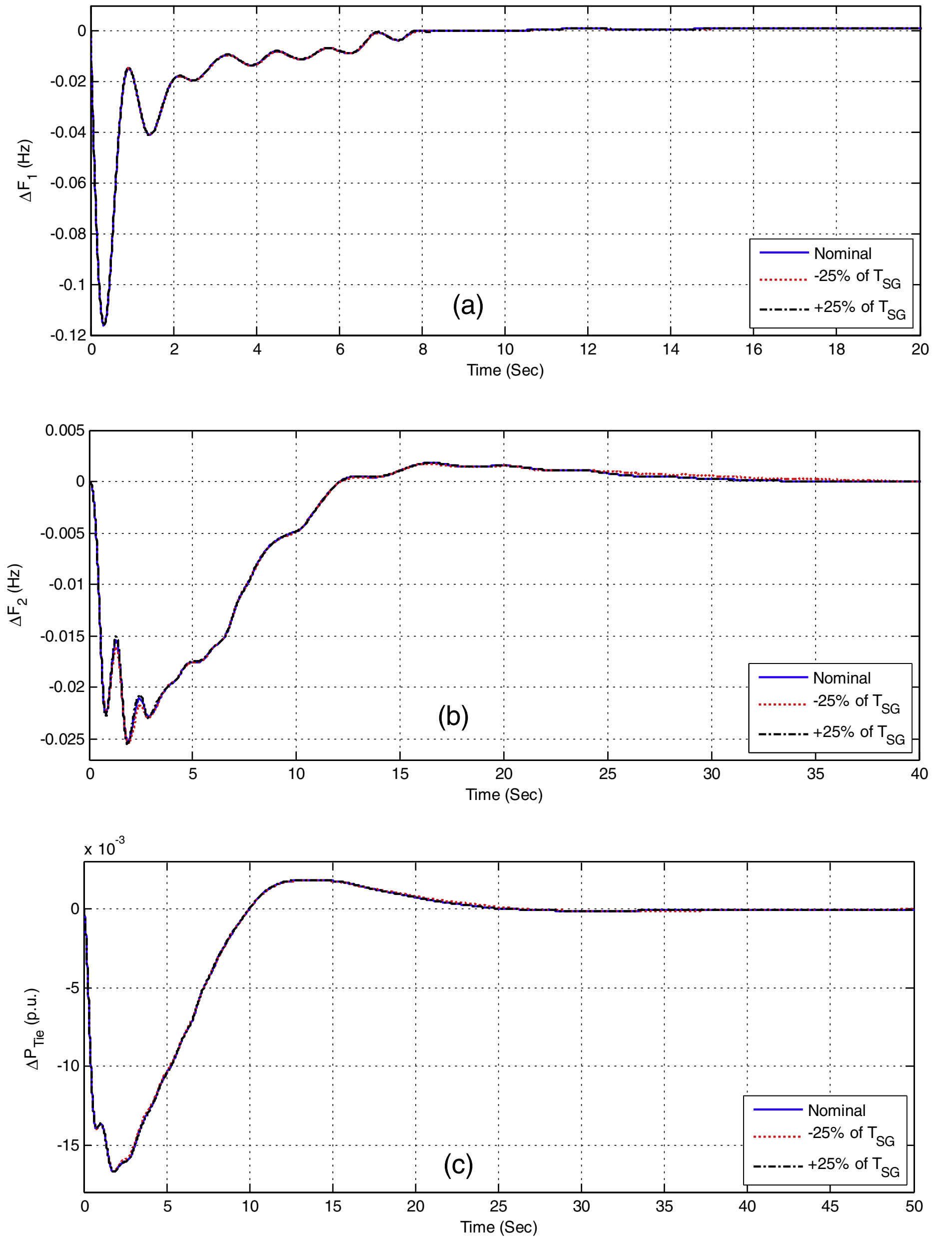

Figure 10 Dynamic responses of the system with variation in T_{SG}. (a) Frequency deviation of area-1. (b) Frequency deviation of area-2. (c) Tie line power deviation.

the one with the better fitness value is admitted to the next generation. The selection operation in DE can be represented by:

$$X_{i,G+1} = \begin{cases} U_{i,G+1} & \text{if } f(U_{i,G+1}) < f(X_{i,G}) \\ X_{i,G} & \text{otherwise.} \end{cases} \quad (14)$$

where $i \in [1, N_P]$.

4. Simulation results and discussion

4.1. Implementation of DE

The model of the system under study shown in Fig. 1 is developed in MATLAB/SIMULINK environment and DE program is written (in .mfile). The LFC in a deregulated power market should be designed to accommodate all possible transactions [6], such as Poolco based transactions, bilateral transactions, and contract violation. Initially, the system without HVDC link is considered and PIDF/fuzzy PIDF controllers are designed for each generating units. The minimum and maximum values of PID controller parameters are chosen as −2.0 and 2.0 respectively. The range for filter coefficient N is selected as 1 and 300 [24]. The developed model is simulated in a separate program (by .mfile using initial population/controller parameters) considering a 10% step load increase in area-1. The objective function is calculated in the .mfile and used in the optimization algorithm. In the present study, a population size of N_P = 100, generation number G = 100, step size FC = 0.8 and crossover probability of CR = 0.8 have been used. The strategy employed is: DE/best/1/exp. Optimization is

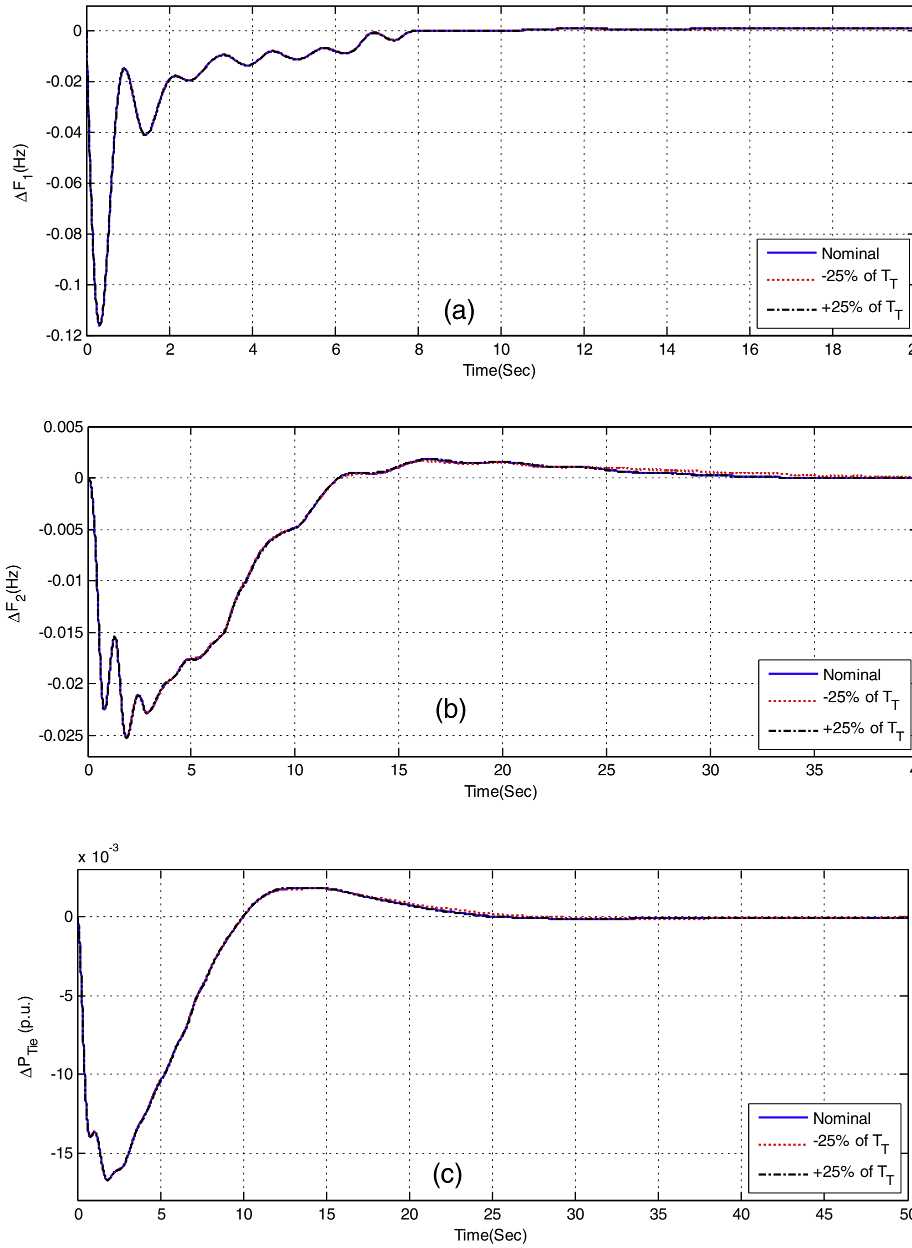

Figure 11 Dynamic responses of the system with variation in T_T. (a) Frequency deviation of area-1. (b) Frequency deviation of area-2. (c) Tie line power deviation.

terminated by the prespecified number of generations for DE. One more important factor that affects the optimal solution more or less is the range for unknowns. For the very first execution of the program, a wider solution space can be given and after getting the solution one can shorten the solution space nearer to the values obtained in the previous iteration. Here the upper and lower bounds of the gains are chosen as (1, −1). The flow chart of the DE algorithm employed in the present study is given in Fig. 5. Simulations were conducted on an Intel, core i-3core CPU, of 2.4 GHz and 4 GB RAM computer in the MATLAB 7.10.0.499 (R2010a) environment. The optimization was repeated 50 times and the best final solution among the 50 runs is chosen as controller parameters.

4.2. Scenario1: Poolco based transaction

In Poolco based transaction, GENCOs participate in LFC of their own control areas only. It is assumed that the load disturbance occurs only in area-1. Thus, the load is demanded only by DISCO1 and DISCO2. For a total load demand of 0.1 (p.u. MW), DISCO1 and DISCO2 demand equally from GENCO1, GENCO2 and GENCO3. So load demands of DISCO1 and DISCO2 are: $\Delta P_{L1} = 0.05$ (p.u. MW), $\Delta P_{L2} = 0.05$ (p.u. MW), $\Delta P_{L3} = \Delta P_{L4} = 0$ as result of the total load disturbance in area-1 is $\Delta P_{D1} = 0.1$ (p.u. MW). A particular case of Poolco based contracts between DISCOs and available GENCOs is simulated based on the following DPM:

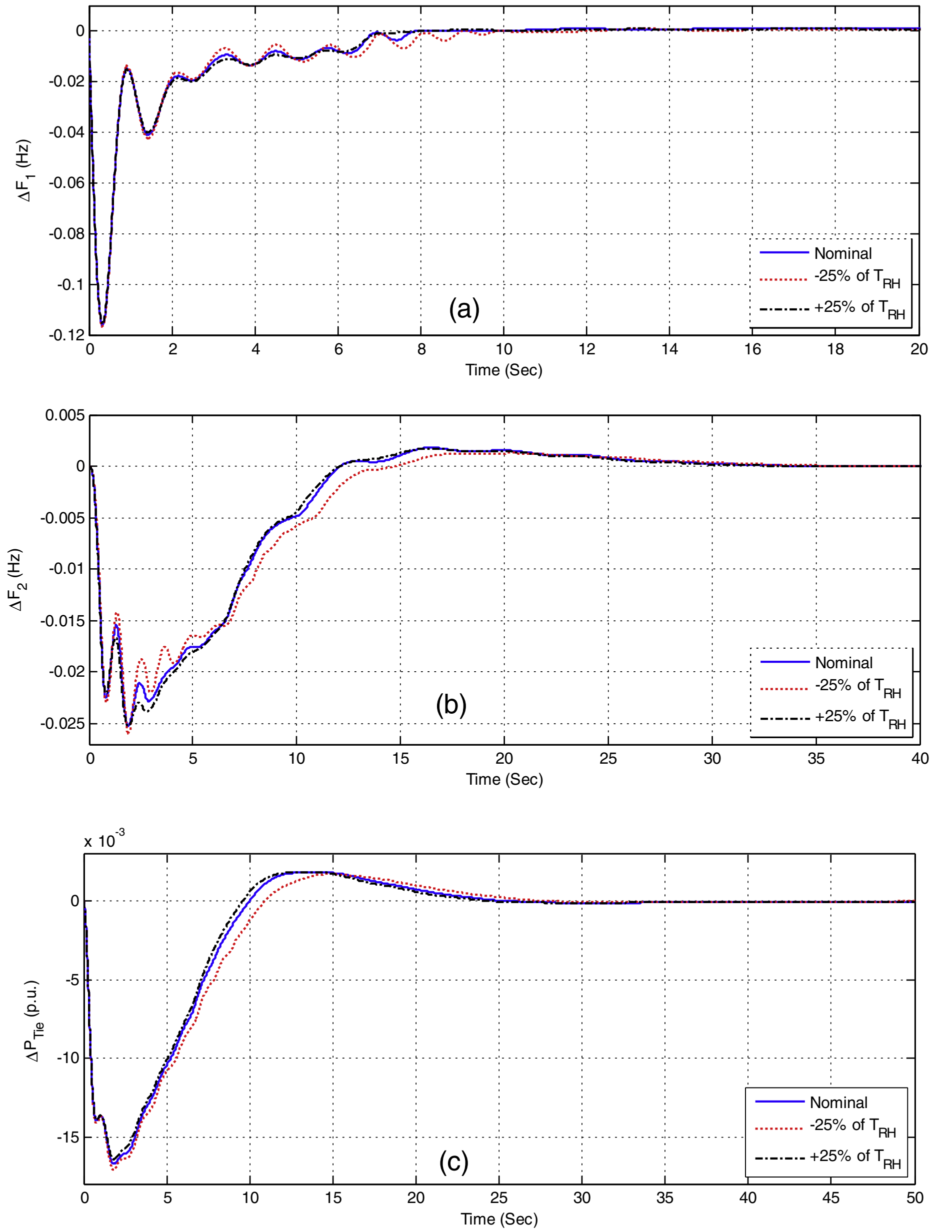

Figure 12 Dynamic responses of the system with variation in T_{RH}. (a) Frequency deviation of area-1. (b) Frequency deviation of area-2. (c) Tie line power deviation.

$$\text{DPM} = \begin{bmatrix} 0.3333 & 0.3333 & 0 & 0 \\ 0.3333 & 0.3333 & 0 & 0 \\ 0.3333 & 0.3333 & 0 & 0 \\ 0 & 0 & 0 & 0 \\ 0 & 0 & 0 & 0 \\ 0 & 0 & 0 & 0 \end{bmatrix} \tag{15}$$

In the above case, DISCO3 and DISCO4 do not demand power from any GENCOs, and hence the corresponding contract participation factors are zero. Accordingly, the ACE participation of GENCOs are: $\text{apf}_{11} = \text{apf}_{21} = 0.6$, $\text{apf}_{12} = \text{apf}_{22} = 0.3$, $\text{apf}_{13} = \text{apf}_{23} = 0.1$.

In the steady state, generation of a GENCO must match the demand of DISCOs in contract with it. The desired generation of the kth GENCO in p.u. MW can be expressed in terms of contract participation factors and the total contracted demand of DISCOs as:

$$\Delta P_{gk} = \text{cpf}_{k1}\Delta P_{L1} + \text{cpf}_{k2}\Delta P_{L2} + \text{cpf}_{k3}\Delta P_{L3} + \text{cpf}_{k4}\Delta P_{L4} \tag{16}$$

where ΔP_{L1}, ΔP_{L2}, ΔP_{L3}, and ΔP_{L4} are the total contracted demands of DISCO1, 2, 3 and 4, respectively.

By using the above equation, the values for ΔP_{g1} can be calculated as:

$$\begin{aligned} \Delta P_{g1} &= \text{cpf}_{11}P_{L1} + \text{cpf}_{12}P_{L2} + \text{cpf}_{13}P_{L3} + \text{cpf}_{14}P_{L4} \\ &= (0.3333) * (0.05) + (0.3333) * (0.05) + (0) * (0) \\ &\quad + (0) * (0) \\ &= 0.03333 \text{ p.u. MW} \end{aligned} \tag{17}$$

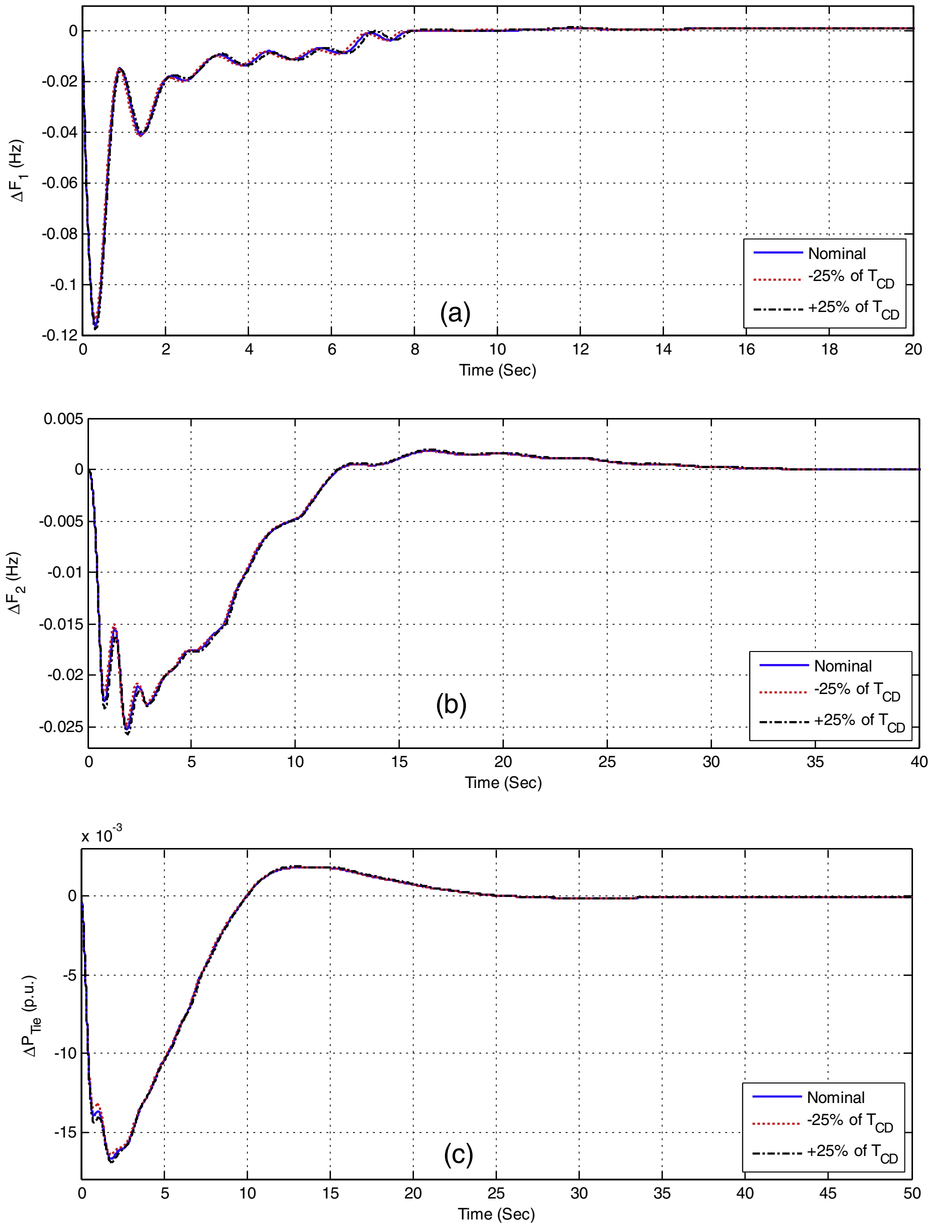

Figure 13 Dynamic responses of the system with variation in T_{CD}. (a) Frequency deviation of area-1. (b) Frequency deviation of area-2. (c) Tie line power deviation.

Similarly, the values of ΔP_{g2}, ΔP_{g3}, ΔP_{g4}, ΔP_{g5} and ΔP_{g6} can be obtained as 0.0333, 0.0333, 0, 0 and 0 p.u. MW respectively.

The final controller parameters for PIDF and fuzzy PIDF controller for the Poolco based transaction are obtained as explained in Section 4.1 and given in Table 2. The performance index values in terms of ITAE value, settling times (2% band), peak overshoot and peak undershoot in frequency and tie line power deviations are shown in Table 3. It is clear from Table 3 that, with the same system (without HVDC) a less ITAE value is obtained with fuzzy PIDF controller (ITAE = 5.0255) compared to PIDF controller (ITAE = 90.3614). Hence it can be conclude that fuzzy PIDF controller outperform PIDF controller. It is clear from Table 3 that the ITAE value is further reduced to 2.3132 when a HVDC link is added to the system. Consequently, better system performance in terms minimum settling times in frequency and tie-line power deviations is achieved with proposed fuzzy PIDF controller for the system with HVDC link compared to other cases as shown in Table 3. It also clear from Table 3 that peak overshoots and undershoots in frequency and tie-line responses are greatly reduced by proposed fuzzy PIDF controller with HVDC. The dynamic performance of the system for 10% step increase in load in area-1 under Poolco based transaction is shown in Fig. 6(a–c). It can be seen from Fig. 6(a–c) that the system is oscillatory with PIDF controller (without HVDC). It is also evident from Fig. 6(a–c) that oscillations are quickly suppressed with proposed fuzzy PIDF controllers and best dynamic performance is obtained by fuzzy PIDF controller with HVDC compared to others.

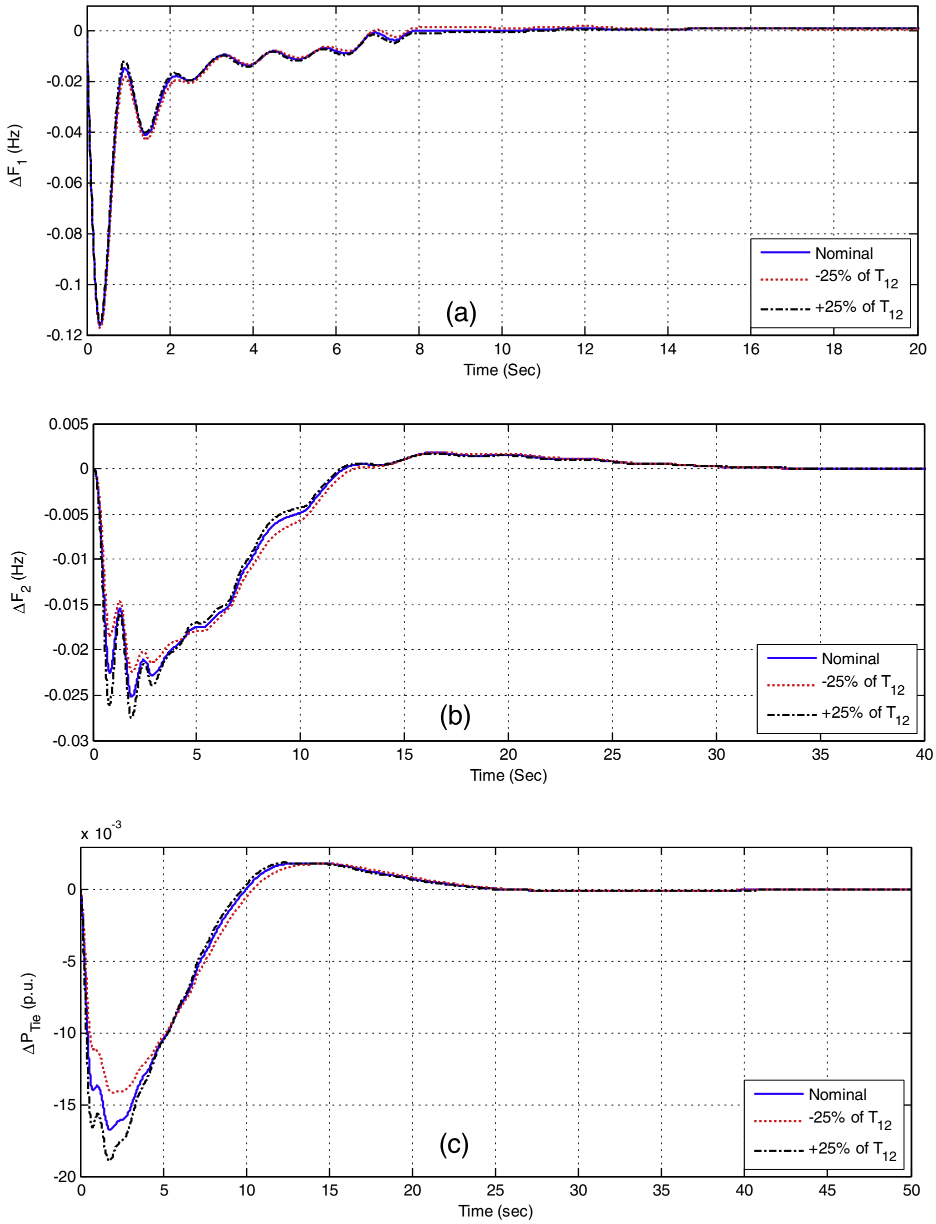

Figure 14 Dynamic responses of the system with variation in T_{12}. (a) Frequency deviation of area-1. (b) Frequency deviation of area-2. (c) Tie line power deviation.

4.3. Scenario2: Bilateral based transaction

In this case, DISCOs have the freedom to contract with any of the GENCOs within own area or with another area. A particular case of Bilateral based transaction is simulated based on the following DPM:

$$\text{DPM} = \begin{bmatrix} 0.2 & 0.1 & 0.3 & 0 \\ 0.2 & 0.2 & 0.1 & 0.1666 \\ 0.1 & 0.3 & 0.1 & 0.1666 \\ 0.2 & 0.1 & 0.1 & 0.3666 \\ 0.2 & 0.2 & 0.2 & 0.1666 \\ 0.1 & 0.1 & 0.2 & 0.1666 \end{bmatrix} \tag{18}$$

In the above case, the load disturbances are 0.05, 0.05, 0.05 and 0.05 p.u. MW in DISCO1, DISCO2, DISCO3 and DISCO4 respectively. From Eq. (7) the values of steady-state power generated by the GENCOs can be obtained as: $\Delta P_{g1} = 0.03$ p.u. MW, $\Delta P_{g1} = 0.03$ p.u. MW, $\Delta P_{g2} = 0.03333$ p.u. MW, $\Delta P_{g3} = 0.03333$ p.u. MW, $\Delta P_{g4} = 0.03668$ p.u. MW, $\Delta P_{g5} = 0.03833$ p.u. MW and $\Delta P_{g6} = 0.02833$ p.u. MW.

The final PIDF and fuzzy PIDF controller parameters for two cases i.e. without HVDC (with only AC line) and with HVDC (both AC–DC parallel lines) are given in Table 4. The corresponding performance index values in terms of ITAE value, settling times (2% band), peak overshoot and peak undershoot in frequency and tie line power deviations are

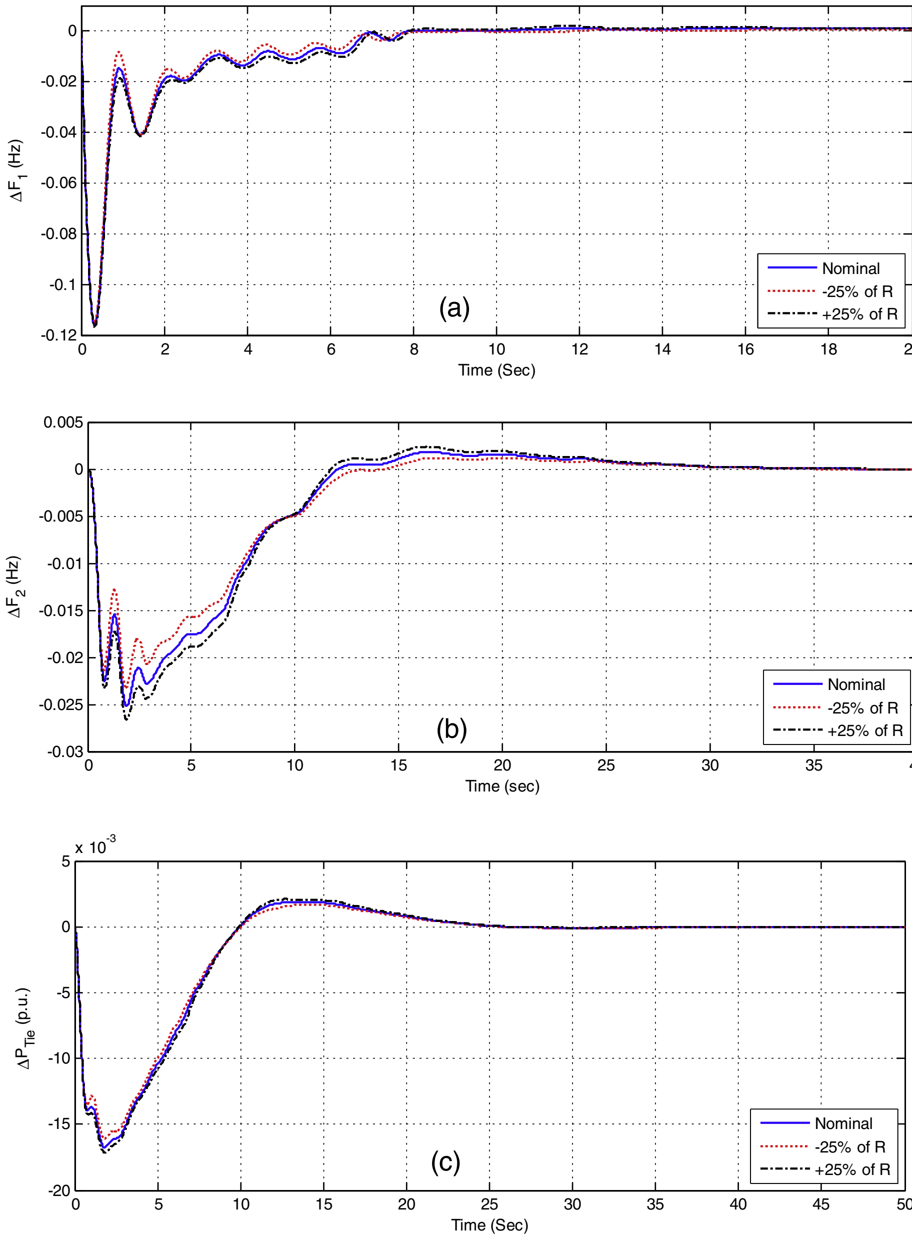

Figure 15 Dynamic responses of the system with variation in R. (a) Frequency deviation of area-1. (b) Frequency deviation of area-2. (c) Tie line power deviation.

shown in Table 5. From Table 5, it is clear that, the smaller ITAE value is obtained with fuzzy PIDF controller (ITAE = 13.19) compared to PIDF controller (ITAE = 69.16). It can be observed from Table 5 that ITAE value is further decreased to 3.28 while considering the HVDC link. Additionally, it can be seen from Table 5 that improved results in settling times of ΔF_1, ΔF_2 and ΔP_{Tie} are obtained with proposed fuzzy PIDF controller (with HVDC) compared to others. The dynamic performance of the system under bilateral based transaction is shown in Fig. 7(a–c). It is clear from Fig. 7(a–c) that better dynamic performance is obtained by fuzzy PIDF controller with HVDC link compared to others.

4.4. Scenario 3: Contract violation based transaction

It may happen that DISCOs may violate a contract by demanding more than that specified in the contract. This excess power is not contracted out to any GENCO. This uncontracted power must be supplied by the GENCOs in the same area as that of the DISCOs. It must be reflected as a local load of the area but not as the contract demand. Considering scenario 2 (bilateral based transaction) again with a modification that 0.01 p.u. MW of excess power demanded by DISCO1. Now ΔP_{D1} becomes 0.11 p.u. MW while ΔP_{D2} remains unchanged. As there is contract violation, the values of ΔP_{g1}, ΔP_{g2} and ΔP_{g3} are to be changed. The change in violation of powers calculated as:

$$\Delta P_{g1,violation} = P_{g1} + \text{apf}_{11} * \Delta P_{violation} = 0.036 \text{ p.u MW} \quad (19)$$

$$\Delta P_{g2,violation} = P_{g2} + \text{apf}_{12} * \Delta P_{violation} = 0.03633 \text{ p.u MW} \quad (20)$$

$$\Delta P_{g3,violation} = 0.03433 \text{ p.u MW.} \quad (21)$$

The values of ΔP_{g4}, ΔP_{g5} and ΔP_{g6} are same as in scenario 2.

Table 6 shows the final PIDF and fuzzy PIDF controller parameters with/without HVDC link. Various performance indexes (ITAE, settling time, peak overshoots and undershoots) under contract violation based transaction case are given in Table 7. It can be seen from Table 7 that improved results are obtained by fuzzy PIDF controller with HVDC link compared to other. The frequency deviations and tie-line power response are shown in Fig. 8(a–c). It is evident from Fig. 8(a–c) that best dynamic response is obtained by proposed fuzzy PIDF controller with HVDC link compared others.

4.5. Sensitivity analysis

Sensitivity analysis is carried out to study the robustness of the system to wide changes in the operating conditions and system parameters [25,26]. Fuzzy PIDF controller with HVDC link is considered in all the cases due to its superior performance. Taking one at a time, the operating load condition, time constants (speed governor time constant T_{SG}, steam turbine constant T_T, hydro turbine speed governor transient droop time constant T_{RH}, gas turbine compressor discharge volume-time constant T_{CD}, tie-line power coefficient T_{12}) and speed regulation parameters (R_{TH}, R_H and R_G for thermal, hydro, gas generating units respectively) are changed from their nominal values (given in Appendix A) in the range of +25% to −25% without changing the optimum values of fuzzy PIDF controller gains. The various performance indexes (ITAE values, settling times and peak overshoot) under normal and parameter variation cases for the system with HVDC link are given in Table 8 under Poolco based transaction. Critical examination of Table 8 clearly reveals that ITAE and settling time values vary within acceptable ranges and are nearby equal to the respective values obtained with nominal system parameter. The dynamic performance of the system with the varied conditions of loading, T_{SG}, T_T, T_{RH}, T_{CD}, T_{12} and R is shown in Figs. 9–15. It can be observed from Figs. 9–15 that the effect of the variation in operating loading conditions and system time constants on the system responses is negligible. So it can be concluded that, the proposed control strategy provides a robust control and the optimum values of controller parameters obtained at the nominal loading with nominal parameters, need not be reset for wide changes in the system loading or system parameters.

5. Conclusions

In this paper, a novel fuzzy PID with derivative filter controller has been proposed for Load Frequency Control (LFC) of an interconnected power system with multi-source power generation in deregulated environment. The study has been conducted on a two area six unit power systems interconnected via parallel AC/DC transmission links. Physical constraints such as Time Delay (TD) and Generation Rate Constraint (GRC) are considered in the system model in order to make the system more realistic and demonstrate the ability of the proposed approach to handle nonlinearity in the system model. Extensive analysis is done for LFC scheme considering Poolco, Bilateral and Contract violation based transaction. DE has been used to optimize the scaling factors and gains of proposed fuzzy PIDF controller employing an ITAE objective function for the above three scenarios and two cases (with/without HVDC link). It is observed that the overall dynamic performance of the system characterized by; ITAE value, settling time, peak overshoots and peak under shoots of the system dynamic response improves remarkably by the use of proposed fuzzy PIDF controller with parallel AC/DC links as an interconnection between the control areas. It is also observed that the designed controllers are robust and perform satisfactorily when the system is subjected to wide variation in loading condition and system parameters.

Appendix A

Nominal parameters of the system investigated.

A.1. Multi-area multi-source power system [12]

$B_1 = B_2 = 0.4312$ p.u. MW/Hz; $R_{TH} = R_{HY} = R_G = 2.4$ Hz/p.u.; $T_{SG} = 0.08$ s, $T_T = 0.3$ s, $K_R = 0.3$; $T_R = 10$ s; $K_{PS} = 73.15$ Hz/p.u. MW; $T_{PS} = 12.19$ s; $T_{12} = 0.0433$, $a_{12} = -1$, $T_W = 1.1$ s, $T_{RS} = 4.9$ s, $T_{RH} = 28.749$ s, $T_{GH} = 0.2$ s, $X_G = 0.6$ s, $Y_G = 1.1$ s, $c_g = 1$, $b_g = 0.049$ s, $T_F = 0.239$ s, $T_{CR} = 0.01$ s, $T_{CD} = 0.2$ s, $K_{DC} = 1.0$, $T_{DC} = 0.2$ s.

The MATLAB program to find out the settling time values for the given system under investigation is provided below.

```
sim('Model',50);
time=[0:0.01:50];
for t=1:5001
  if (Del_f_1(t)>=0.002|| Del_f_1(t)<=-0.002)
    st=t;
  end
end
Settling_Time_for_Delf_1=time(st)% Computes the settling time
```

References

[1] Elgerd OI. Electric energy systems theory – an introduction. New Delhi: Tata McGraw Hill; 2000.

[2] Kundur P. Power system stability and control. 8th reprint. New Delhi: Tata McGraw-Hill; 2009.

[3] Bevrani Hassan. Robust power system frequency control. Springer; 2009.

[4] Bervani Hassan, Hiyama Takashi. Intelligent automatic generation control. CRC Press; 2011.

[5] Ibraheem, Nizamuddin, Bhatti TS. AGC of two area power system interconnected by AC/DC links with diverse sources in each area. Int J Elect Power Energy Syst 2014;55:297–304.

[6] Donde V, Pai MA, Hiskens IA. Simulation and optimization in an AGC system after deregulation. IEEE Trans Power Syst 2011;16:481–9.

[7] Bhatt P, Roy R, Ghoshal SP. Optimized multi-area AGC simulation in restructured power systems. Int J Electr Power Energy Syst 2010;32(4):311–22.
[8] Tyagi B, Srivastava SC. A decentralized automatic generation control scheme for competitive electricity markets. IEEE Trans Power Syst 2006;21(1):312–20.
[9] Christie RD, Bose A. Load frequency control issues in power system operation after deregulation. IEEE Trans Power Syst 1996;11(3):1191–200.
[10] Tan W, Zhang H, Yu M. Decentralized load frequency control in deregulated environments. Int J Elect Power Energy Syst 2012;41:16–26.
[11] Chidambaram IA, Paramasivam B. Optimized load-frequency simulation in restructured power system with Redox Flow Batteries and Interline Power Flow Controller. Int J Electr Power Energy Syst 2013;50:9–24.
[12] Parmar KPS, Majhi S, Kothari DP. LFC of an interconnected power system with multi-source power generation in deregulated power environment. Int J Electr Power Energy Syst 2014;57:277–86.
[13] Mudi KR, Pal RN. A robust self-tuning scheme for PI-and PD-type fuzzy controllers. IEEE Trans Fuzzy Syst 1999;7(1):2–16.
[14] Mudi KR, Pal RN. A self-tuning fuzzy PI controller. Fuzzy Sets Syst 2000;115(2):327–88.
[15] Yesil E, Guzelkaya M, Eksin I. Self tuning fuzzy PID type load and frequency controller. Energy Convers Manage 2004;45(3):377–90.
[16] Panda S. Differential evolution algorithm for SSSC-based damping controller design considering time delay. J Franklin Inst 2011;348(8):1903–26.
[17] Saikia LC, Mishra S, Sinha N, Nanda J. Automatic generation control of a multi area hydrothermal system using reinforced learning neural network controller. Int J Elect Power Energy Syst 2011;33(4):1101–8.
[18] Woo ZW, Chung HY, Lin JJ. A PID type fuzzy controller with self-tuning scaling factors. Fuzzy Sets Syst 2000;115(2):321–6.
[19] Visioli A. Tuning of PID controllers with fuzzy logic. IEE Proc Control Theory Appl 2001;48(1):1–8.
[20] Das S, Pan I, Das S, Gupta A. A novel fractional order fuzzy PID controller and its optimal time domain tuning based on integral performance indices. Eng Appl Artif Intell 2012;25:430–42.
[21] Sahu RK, Panda S, Padhan S. Optimal gravitational search algorithm for automatic generation control of interconnected power systems. Ain Shams Eng J 2014;5(3):721–33.
[22] Shabani H, Vahidi B, Ebrahimpour M. A robust PID controller based on imperialist competitive algorithm for load-frequency control of power systems. ISA Trans 2013;52(1):88–95.
[23] Storn R, Price K. Differential evolution – a simple and efficient adaptive scheme for global optimization over continuous spaces. J Global Opt 1995;11:341–59.
[24] Tan W. Unified tuning of PID load frequency controller for power systems via IMC. IEEE Trans Power Syst 2010;25(1):341–50.
[25] Rout UK, Sahu RK, Panda S. Design and analysis of differential evolution algorithm based automatic generation control for interconnected power system. Ain Shams Eng J 2013;4(3):409–21.
[26] Panda S, Yegireddy NK, Mahapatra S. Hybrid BFOA–PSO approach for coordinated design of PSS and SSSC-based controller considering time delays. Int J Elect Power Energy Syst 2013;49:221–33.

Rabindra Kumar Sahu received the Ph.D. degree from the Indian Institute of Technology (IIT) Madras, Chennai, India. He is currently working as Associate Professor in the Department of Electrical Engineering, Veer Surendra Sai University of Technology (VSSUT), Burla, Sambalpur, Odisha, India. His research interests include application of soft computing techniques to power system engineering, Flexible AC Transmission Systems (FACTS). Dr. Sahu is life member of ISTE.

G.T. Chandra Sekhar received B.Tech degree in EEE from St. Theressa Institute of Engineering & Technology, Vizianagaram affiliated to JNTU, Hyderabad, Andhra Pradesh in 2008. M.Tech Degree in EEE from St. Theressa institute of Engineering & Technology, Vizianagaram affiliated to JNTU, Kakinada, Andhra Pradesh in 2011. He is currently working toward the Ph.D. degree at the Department of Electrical Engineering, VSSUT, Burla, Odisha, India. His research interests include soft computing application in power system Engineering. Mr. Chandra Sekhar is life member of ISTE.

Sidhartha Panda received Ph.D. degree from Indian Institute of Technology (IIT), Roorkee, India, M.E. degree from Veer Surendra Sai University of Technology (VSSUT). Presently, he is working as a Professor in the Department of Electrical Engineering, Veer Surendra Sai University of Technology (VSSUT), Burla, Sambalpur, Odisha, India. His areas of research include Flexible AC Transmission Systems (FACTS), Power System Stability, Soft computing, Model Order Reduction, Distributed Generation and Wind Energy. Dr. Panda is a Fellow of Institution of Engineers (India).